Received May 16, 2020, accepted May 26, 2020, date of publication June 2, 2020, date of current version June 12, 2020.

Digital Object Identifier 10.1109/ACCESS.2020.2999338

Wide-Angle Frequency Scanning Metasurface Antenna Fed by Spoof Plasmonic Waveguide

HONGYA CHEN[1], YAJUAN HAN[2], HUA MA[1], JIAFU WANG[1], (Member, IEEE), AND MINGBAO YAN[1]

[1]College of Science, Air Force Engineering University, Xi'an 710051, China
[2]School of Physics and Optoelectronic Engineering, Xidian University, Xi'an 710051, China

Corresponding authors: Hua Ma (mahuar@163.com) and Jiafu Wang (wangjiafu1981@126.com)

This work was supported in part by the National Natural Science Foundation of China under Grant 61601507, Grant 61671467, and Grant 61971435, in part by the National Key Research and Development Program of China under Grant 2017YFA0700201, and in part by the Natural Science Foundation of Shaanxi Province under Grant 2020JM-351.

ABSTRACT We propose novel wide-angle frequency scanning metasurface antenna and antenna array fed by spoof plasmonic waveguide. The spoof plasmonic waveguide adopts the ultra-thin corrugated metallic strip which can support and propagate spoof surface plasmon polariton (SSPP) with high efficiency. By compensating the momentum difference between SSPP and free-space propagation modes via constant phase gradient, metasurface antenna can exhibit wide-angle and continuous radiation property according to the Generalized Snell's law. A prototype is designed, fabricated and measured, which consists of a wideband polarization rotating transmissive phase gradient metasurface (TPGM) placed a certain distance above spoof plasmonic waveguide. Such antenna works in a wideband range from 6.8 to 14.0 GHz, and the main beam can continuously scan from the forward direction to the backward direction with high efficiency. The measured results show that the scanning angle can reach 55°, which agree well with the simulated and theoretically calculated results. Furthermore, the proposed metasurface antenna can be combined easily as an antenna array with a simple feed network. Compared to single metasurface antenna, the antenna array exhibits the pencil-shaped directional radiation property, and the average gain of antenna array is obviously enhanced. The proposed frequency scanning metasurface antenna is of great value in the design of conformal antenna and the large aperture antenna array, especially on curved faces.

INDEX TERMS Spoof surface plasmon polaritons, transmissive phase gradient metasurface, frequency scanning, antenna array.

I. INTRODUCTION

Surface plasmon polaritons (SPPs) are highly localized electromagnetic (EM) wave bounded along an interface of metal and dielectric medium at the optical frequency band [1], [2]. Due to their unique properties of field enhancement and energy localization in sub-wavelength scales, SPPs have important potential applications in super resolution imaging, bio-sensing, photonics, etc [3]–[5]. However, SPPs cannot be excited effectively on flat metallic plate at lower frequencies. To overcome this obstacle, artificial structured surfaces decorated by periodic grooves, slits, or holes have been studied to support and propagate spoof SPPs (SSPPs), which have similar properties of SPPs at optical frequencies [6]–[9]. Recently, the ultra-thin corrugated metallic strip (CMS) fed by a coplanar waveguide has been investigated by both simulation and experiment, which can realize broadband and high-efficiency conversion from the guided wave to SSPPs [10], [11]. Phase gradient metasurface can also convert a propagating wave into SSPP via pre-defining wave vector along the surface [12], [13]. Especially, SSPP meta-coupler based on a transmissive phase gradient metasurface (TPGM) can convert the incident propagating wave to the eigen-mode SSPP with high conversion efficiency of 73% according to the near-field and far-filed experiment, which can suppress both decoupling and surface initial reflections [14], [15].

According to the principle of reversibility, SSPPs can also be converted into free-space radiation, which has potential applications in leaky-wave antennas [16]–[21], [25]–[29]. Continuous beam scanning leaky-wave antenna can be

The associate editor coordinating the review of this manuscript and approving it for publication was Lin Peng.

achieved by circular patches loaded periodically along one side of the SSPP transmission line. That is because it can achieve an additional momentum to modulate the SSPP wave into a spatial wave [11], [16]. Cui *et al* demonstrated that periodically-modulated spoof plasmonic waveguide structures composed of non-uniform CMS have the ability of converting SSPPs to spatial wave [17]. Recently, a wide-angle frequency scanning antenna is proposed based on a hybrid mode of a quasi-TEM mode and a SSPPs mode [18]. The wide-range scanning in a narrower band can be realized due to the nonlinear dispersion curve of SSPPs [18]–[21]. However, above antennas cannot modulate polarization characteristic. Phase gradient metasurface is a two-dimensional planar array composed of sub-wavelength element structure, which can freely control the polarization mode, wave-front, propagation direction, propagation mode [22]–[24]. Therefore, it also can use the phase gradient as an additional momentum for converting the slow-wave mode to a fast-wave mode and then to modulate the SSPPs to radiation wave. In 2015, Cui *et al* have achieved efficient conversion of surface-plasmon-like modes to spatial radiated modes by controlling phase modulations produced by the reflective phase gradient metasurface (RPGM) [25], [26]. Qu *et al* have also proposed a frequency scanning antenna by decoupling SSPP via RPGM [27], [28]. The radiation angles are modulated by both the nonlinear phase gradient and the wave vector of SSPP. In order to achieve wideband frequency scanning characteristic and higher efficiency, SSPP planar antenna based on wideband TPGM is proposed [29]. The antenna consists of TPGM placed a certain distance above an SSPP guided wave structure. In addition, it has a polarization conversion characteristic by using polarization conversion TPGM as both the radiating and receiving panel. However, this antenna is also fed by rectangular waveguide, which will lead to a larger antenna profile and feeding structure in lower frequency regime, especially in the meter-wave regime. Furthermore, the dispersion of SSPP on the metallic grating structure cannot be modulated flexibly by changing parameters of the metallic grating structure, which will limit the working bandwidth and scanning range.

In this paper, we propose an alternative method for designing frequency scanning metasurface antenna fed by spoof plasmonic waveguide. The configuration of such antenna is composed of a TPGM placed a certain distance above a spoof plasmonic waveguide. The spoof plasmonic waveguide adopts the CMS fed by coplanar waveguide here and the dispersion of SSPP on CMS can be controlled easily by height of strip. By compensating the differences between wave vector of SSPP on the ultra-thin CMS and spatial propagating modes by using transmissive phase gradient, the SSPP can be converted to directional radiation. Compared to the existing planar leaky-wave antenna, our antenna has several advantages. Firstly, since the radiation angles are mainly regulated by the nonlinear dispersion of SSPP on CMS and wideband phase gradient, it can be easier to realize a continuous wide-angle and wideband frequency scanning.

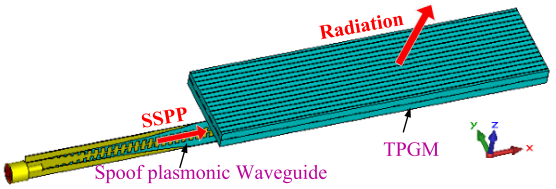

FIGURE 1. The schematic diagram of metasurface antenna.

Secondly, it has a polarization conversion characteristic by using polarization conversion metasurface. Thirdly, owing to low loss, low profile and simple fabrication, the method also possesses potential applications in plasmonic waveguide communication. Lastly, since the TPGM doesn't need the electrical connection, it is easy to combine the large aperture antenna array with simple feed network. To verify this idea, wide-angle and wideband directional radiation antenna and antenna array are designed and measured by using wideband linear polarization conversion TPGM as radiated panel. Both simulated results agree well with the measured results.

II. DESIGN PRINCIPLE

The working principle of our designed frequency scanning metasurface antenna is based on transmissive phase gradient modulation on eigen-mode SSPP. In essence, SSPPs are non-radiative EM modes, whose wave vector k_{sspp} is larger than that in free space k_0. The SSPP mode can be converted into a radiated mode when wave vector of SSPPs is reduced to radiation region under certain conditions. Fortunately, TPGM can provide pre-defined phase gradient on the surface, which can compensate the wave vector difference between k_{sspp} and k_0 at the same frequency. That means perfect momentum matching can be achieved. According to the working principle analyzed above, the schematic diagram of metasurface antenna is shown in Fig. 1, which consists of TPGM and spoof plasmonic waveguide. Here, the spoof plasmonic waveguide also adopts the CMS fed by coplanar waveguide. It has been demonstrated that waves on CMS have similar EM behavior as TM-mode SSPPs [10]. According to the generalized Snell's law [22], the radiation angle of frequency scanning antenna can be calculated by a formula as [26]–[28]

$$\theta = \arcsin\left(\frac{k_{sspp} - \xi}{k_0}\right) \tag{1}$$

where the ξ is the transmissive phase gradient. The radiation angle is mainly controlled by the nonlinear dispersion of SSPP on the CMS and phase gradient generated by TPGM, both of which can be designed separately. Therefore, a wideband and wide-angle beam scanning from backward to forward can be easily achieved by elaborate designing of CMS and phase gradient ξ.

III. DESIGN OF FREQUENCY SCANNING METASURFACE ANTENNA

A. DESING OF TRANSMISSIVE PHASE GRADIENT METASURFACE

In order to validate this idea, we design a wide-angle and wideband frequency scanning metasurface antenna. For

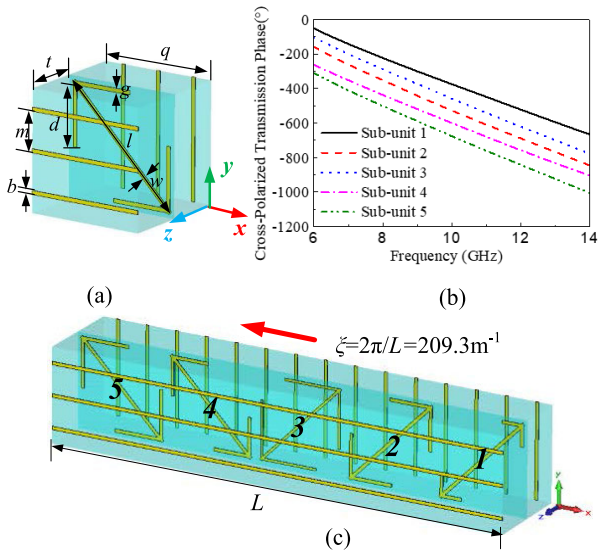

FIGURE 2. Design of the linear polarization conversion TPGM: (a) geometric parameters of transmissive sub-unit cell (b) cross-polarized transmission phase for a *y* -polarized normally incident EM wave, (c) the super cell composed of five sub-unit cells.

comparison to SSPP planar antenna fed by rectangular waveguide [29], we adopt the same TPGM as radiated panel. Such TPGM can generate wideband and constant phase gradient along the x direction from $f = 6.8$ GHz to 14 GHz [15]. As shown in Figure 2(a), the sub-unit cell is composed of two-layer F4B dielectric ($\varepsilon_r = 2.65$, $\tan\delta = 0.001$, $t = 3$mm) and three metallic layers. When the y-polarized wave normal incidence, it can efficiently convert into wideband x-polarized transmission wave due to both multiple plasmon resonances and Fabry-Perot-like resonances [30]. Here five different sub-unit cells are selected to construct the super cell. The optimized parameters of the super cell are (l, d, g) = (7.7mm, 1.2mm, 0.2mm), (7.7mm, 2.6mm, 0.2mm), (7.5mm, 3.55mm, 0.15mm), (7.6mm, 2.3mm, 0.2mm), (7.8mm, 3mm, 0.2mm), respectively. The other parameters are the same with $q = 6$mm, $m = 2$mm, $b = 0.2$mm and $w = 0.2$mm. Figure 2(b) shows the cross-polarized transmission phase for a y-polarized normally incident EM wave. It can be clearly seen that the phase change step is $2\pi/5$ along each sub-unit cell from 6.8 to 14.0 GHz. Therefore, these five sub-unit cells compose a super cell to realize 2π phase change and the phase gradient can be calculated as $\xi = 2\pi/L = 209.3\ \mathrm{m}^{-1}$. In order to generate phase gradient along the $-x$ direction, the 5 sub-unit cells are arranged in reverse to that of Ref [15], as shown in Fig.2(c). Since the phase gradient can hold nearly constant in a wide frequency range, the radiation angles are mainly modulated by the dispersion of SSPP, which is different to Ref [27], [28]. The total size of the TPGM here is set to be 300 mm×30 mm, consisting of 10 super unit cells along x axis and 5 unit cells along y axis.

B. DESING OF SPOOF PLASMONIC WAVEGUIDE

The spoof plasmonic waveguide is carefully designed, as shown in Fig.3, which has a similar structure as discussed in Ref [10]. It has been confirmed to be able of converting the guided EM wave to SSPPs in a wideband with high efficiency due to good momentum and impedance matching. The spoof plasmonic waveguide consists three parts, in which $l_1 = 8$ mm, $l_2 = 56$ mm, and $l_3 = 300$ mm. The whole spoof plasmonic waveguide is printed on flexible dielectric substrate F4B ($\varepsilon_r = 2.65$ and $\tan\delta = 0.001$) with the thickness 0.2mm. Note that the spoof plasmonic waveguide does not have metallic back sheet.

The part I is the coplanar waveguide as shown in Fig. 3(b), which is designed to achieve 50Ω impedance with the dimensions $w_c = 3$ mm, $g_c = 0.25$ mm, and $h_c = 4.7$ mm. The part II is the transition with gradient grooves and flaring ground to achieve good momentum and impedance matching as shown in Fig.3(c), in which $h_1 = 0.225$ mm, $h_2 = 0.45$ mm, $h_3 = 0.675$ mm, $h_4 = 0.9$ mm, $h_5 = 1.125$ mm, $h_6 = 1.35$mm, $h_7 = 1.575$ mm, $h_8 = 1.8$ mm, and $h_9 = 1.9$ mm, respectively. The curve of flaring ground is described as

$$y = C_1 e^{\alpha x} + C_2 \ (x_1 < x < x_2)$$

where $C_1 = (y_1 - y_2)/(e^{\alpha x_2} - e^{\alpha x_1})$, $C_2 = (y_2 e^{\alpha x_1} - y_1 e^{\alpha x_2})/(e^{\alpha x_1} - e^{\alpha x_2})$ $\alpha = 0.05$, and (x_1, y_1) and (x_2, y_2) are the start and end points of the curve.

The part III is the double-side CMS without the metallic back is shown in Fig. 3(a) and inset of Fig. 3(d). The desired dispersion relation of CMS for the TM-polarized waves propagating along the x direction can be approximately obtained as following [10]:

$$k_{sspp} = k_0 \sqrt{1 + \frac{a^2}{p^2} \tan^2(k_0 h)} \tag{2}$$

where p, a, and h are the period, width, and depth of the grooves, respectively. When $0 < k_0 h < \pi/2$, k_{sspp} shall be a real number and $k_{sspp} > k_0$. Hence, the dispersion relation of SSPP on the CMS can be easily tuned by the depth of grooves. Thus, propagation characteristics of SSPP on CMS can be manipulated easily through changing the depth of grooves h. Here, the parameters of CMS are set to $p = 2.5$mm, $a = 1.0$ mm, $h = 1.9$mm and $s = 0.9$mm, respectively. Figure 3(d) gives dispersion curves of SSPP on the CMS and TPGM-modulated CMS, respectively. As shown in Fig. 3(d), the red curve shows the dispersion relation of SSPP on the CMS, while the black curve gives the dispersion relation in free space. It can be seen that the wave vector of SSPP k_{sspp} is much larger than that of the free space k_0. The constant phase gradient ξ designed along $-x$ direction can compensate momentum difference between the SSPP and propagating waves. The blue curve shows the dispersion of SSPP on the modulated CMS by the transmissive phase gradient ξ. Within the band of 6.8-14.0 GHz, the modulated dispersion relation (blue curve) is shifted from the slow-wave region to the fast-wave region (the green zone), which means the SSPPs on the CMS can be decoupled to directional radiation wave in this region according to the generalized Snell's law. Here, only

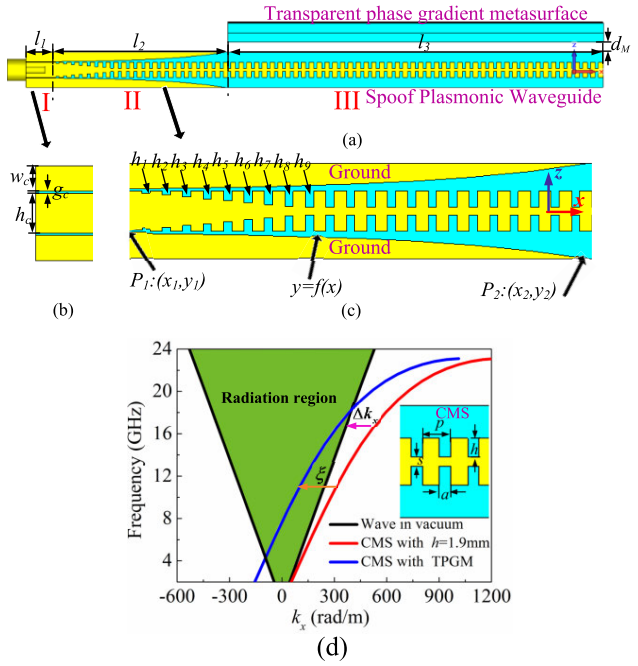

FIGURE 3. Design of the spoof plasmonic waveguide: (a) the profile of frequency scanning metasurface antenna, (b) coplanar waveguide section, (c) The matching transition with gradient grooves and flaring ground, (d) dispersion curves of SSPP on the CMS and TPGM-modulated CMS, respectively. The inset is design of ultrathin CMS without the metallic back.

zero-order dominant mode of SSPP dispersion is utilized to realize the desirable radiation [28]. It can also be seen that our antenna has the capability of scanning from backfire to endfire.

Since waves on CMS have similar EM behavior as TM-mode SSPPs with E-field mainly distributed in the *xoz* plane [10], [28], the TPGM is placed above the spoof plasmonic waveguide with a certain distance for the mode matching. The distance is set to $d_M = 1.6$ mm by optimization.

C. RESULTS AND ANALYSIS

We carry out both simulation and experiment to verify the properties of metasurface antenna designed above. The simulations are carried out by using Computer Simulation Technology (CST) Microwave Studio. Fig.4(a) illustrates the sample of whole antenna and the inset view shows TPGM and spoof plasmonic waveguide structures in detail. As can be seen from the front view of the sample, the spoof plasmonic waveguide is placed in the middle of the TPGM. Simulated and measured results of the reflection coefficient are shown in Fig.4(b). In the 6.8-14.0 GHz frequency range, S_{11} is nearly lower than -10 dB, which means that most energy of SSPP is radiated out. The experimental result is almost in agreement with the simulated one and the little deviation may result from fabrication and measurement error.

In order to further verify the working principle of the metasurface antenna, we monitor the near-field and far-field distribution of the antenna at $f = 10.0$ GHz as shown in Fig.5. From the electric field E_z distribution shown in

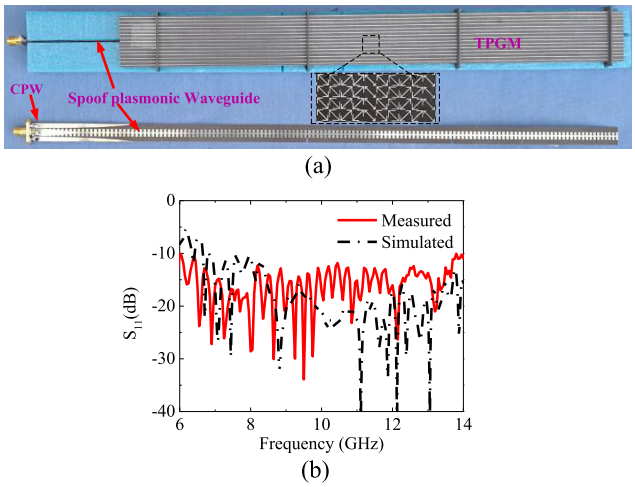

FIGURE 4. (a) Sample of whole frequency scanning metasurface antenna, (b) simulated and measured reflection coefficient S_{11}.

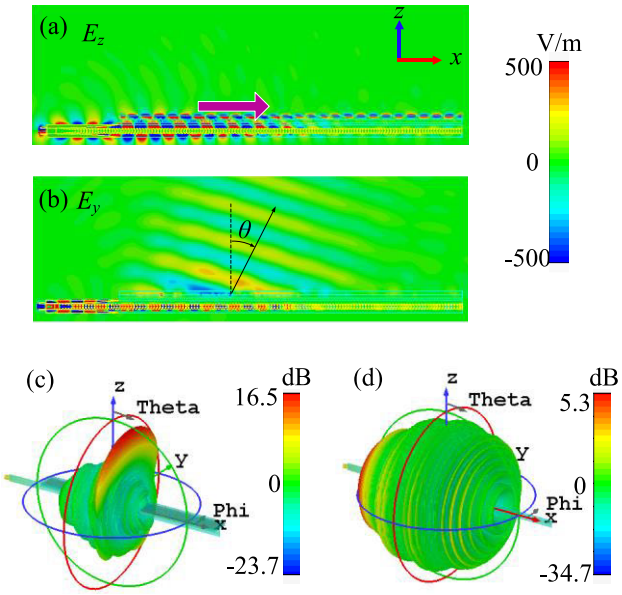

FIGURE 5. Simulated results of near-field and far-field distribution of metasurface antenna at $f = 10$GHz, (a) E_z, (b) E_y, (c) simulated 3D radiation realized gain pattern of metasurface antenna, (d) simulated 3D radiation realized gain pattern of antenna without TPGM above the spoof plasmonic waveguide.

Fig.5(a), we observe that incident EM wave is firstly coupled to high-efficiency TM-mode SSPPs with the E-field mainly distributed in the *xoz* plane and then the SSPPs propagate along the CMS. When SSPPs transmit to the TPGM, the high-efficiency directional radiations are generated by gradually decoupling SSPP on the CMS by phase gradient. In addition, since we use the linear polarization rotation TPGM as the radiated panel, the TM-mode SSPP finally converts into the *y* polarization radiated wave with the radiation angle of 16° at $f = 10$ GHz. This can be validated by electric field E_y distribution shown in Fig.5(b). Fig.5(c) and (d) show the 3D radiation realized gain pattern of metasurface antenna and antenna without the TPGM above the spoof plasmonic waveguide. By comparison, it can be seen obviously that the

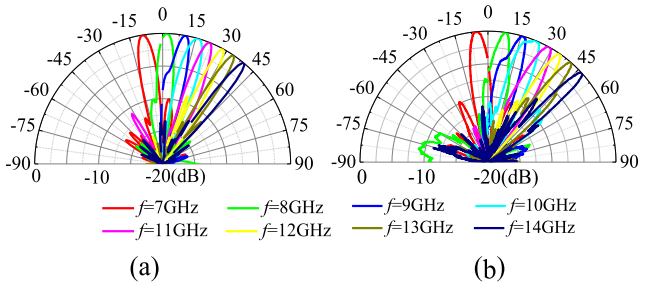

FIGURE 6. Simulated and measured normalized H-plane radiation patterns at different frequencies.

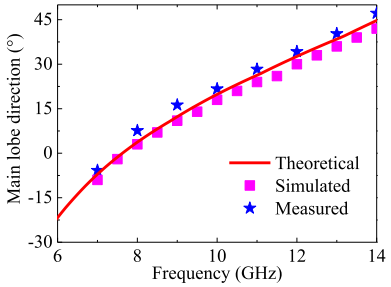

FIGURE 7. H-plane main lobe direction of antenna obtained by theoretical calculation, simulation and measure, respectively.

high-efficiency directional radiation is achieved with the peak realized gain of 16.5 dB by metasurface antenna as shown in Fig.5(c).

We have also simulated and measured normalized H-plane radiation patterns at different frequencies as shown in Fig. 6. It can be seen that the main lobe in the H-plane can continuously steer from backward to forward as frequency changes from 6.8 GHz to 14.0 GHz, which proves that SSPP can be decoupled to directional radiation wave. The measured results agree well with the simulated results. Fig. 7 presents H-plane main lobe direction of antenna obtained by theoretical calculation (red line), simulation (black line) and measure (blue star), respectively. The theoretical calculation is based on Eq. (1) by using dispersion relation of SSPP on CMS with $h = 1.9$ mm as shown in Fig. 3(d). It can be seen from the theoretical calculation that the antenna is capable of scanning from $-10°$ to $45°$ in the frequency range of 6.8-14.0 GHz, which is in good agreement with the measured and simulated results.

Fig. 8 shows simulated results of the peak gain curve, radiation efficiency and total efficiency of the designed metasurface antenna in the band of 6.8-14.0 GHz, respectively. As can be seen from Fig. 8(a), the average gain of the SSPP planar antenna is 15.8 dB and the maximal gain reaches 17.9 dB at $f = 12$ GHz. As can be seen from Fig. 8(b), the total efficiency and radiation efficiency of designed antenna are greater than 80%, with the maximal total efficiency of 92%, which is higher than that of the beam scanning of patch array in Ref [11]. Hence, the designed antenna has properties of high gain and high efficiency.

IV. METASURFACE ANTENNA ARRAY

As we can see from Fig.2(c), sub-unit cells of TPGM as the radiated panel do not require the electrical connection, they

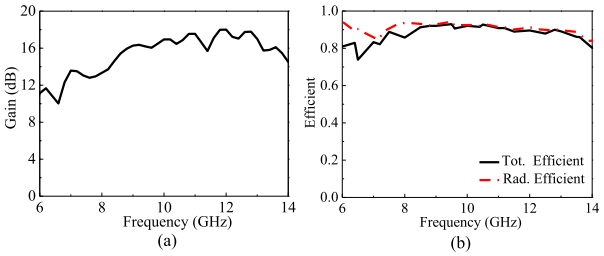

FIGURE 8. Simulated results of frequency scanning metasurface antenna (a) peak gain curve, (b) the radiation efficiency and total efficiency.

can be divided and assembled easily. Therefore such antenna is convenient for transportation and application. Inspired for this, we can combine some single metasurface antennas to an array with a simple feed network. To validate this idea, we use eight identical metasurface antennas designed above (marked as A-1) to assemble an array along y axis, as shown in Fig.9(a) (marked as A-8). The sample of metasurface antenna array A-8 is shown in Fig.9(b), which has a larger size of 300 mm×240 mm, consisting of 10 super-unit cells along x axis and 40 unit cells along y axis. The antenna array is fed individually by eight spoof plasmonic waveguides. And the spoof plasmonic waveguides are fed simultaneously by eight coplanar waveguides. Therefore there is no mutual couple between the ports. The SSPP can also be decoupled by TPGM. According to antenna array theory, the radiation pattern of uniformly linear antenna array depends on the array pattern. Its normalized array pattern can be expressed as

$$F(\psi) = \frac{\sin(N\psi/2)}{N\sin(\psi/2)} \tag{3}$$

where ψ denotes phase difference in the radiation of adjacent units and N denotes the number of unit antenna. According to Eq. (3), the larger the number of unit antenna N, the narrower the radiated beam of antenna array becomes. The simulated and measured results of the reflection coefficients are shown in Fig.9(c). The simulated S-parameters are all nearly lower than -10 dB in the 6.8-14.0 GHz frequency range, the bandwidth of which are the same with the single antenna A-1. Note that the S-parameters have little difference to each other due to the less mutual near-field coupling. The measured result agrees with the simulated ones. We also monitor the far-field radiation of the antenna array at $f = 10$ GHz as shown in Fig.9(d). We can see that the radiation pattern of antenna array changes from sector-shaped to pencil-shaped compared to single antenna A-1 as shown in Fig.5(c). High-efficiency directional radiation is achieved due to antenna array along y axis. The peak of realized gain enhances to 26.2 dB, which is higher than that of the single antenna A-1 with 9.7 dB at $f = 10$ GHz. Therefore the gain can be further improved by antenna array.

Fig.10 gives the H-plane main lobe direction results of metasurface antenna A-1 and antenna array A-8 by simulation and measure, respectively. It can be seen obviously that the directional radiation angles of antenna array A-8 follow the Generalized Snell's low. Besides, the radiation angles of

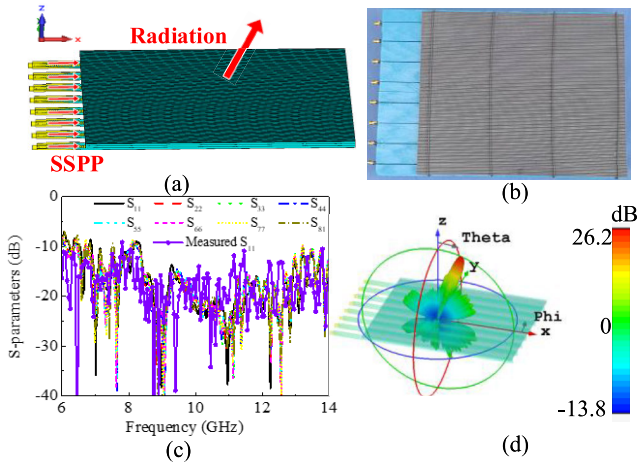

FIGURE 9. Metasurface antenna array, (a) 3D view, (b) sample, (c) simulated and measured reflection coefficients, (d) simulated 3D radiation realized gain pattern at $f = 10$ GHz.

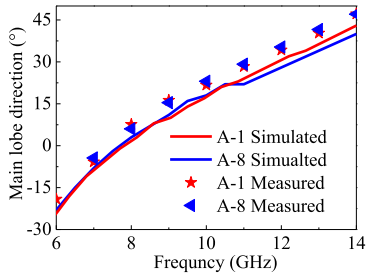

FIGURE 10. H-plane main lobe direction of metasurface antenna A-1 and metasurface antenna array A-8 by simulation and measure, respectively.

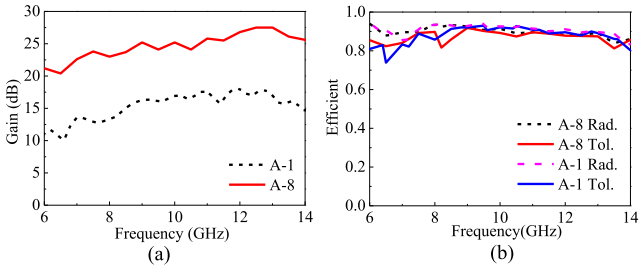

FIGURE 11. (a) Peak gain curve of metasurface antenna A-1 and metasurface antenna array A-8, (b) the radiation efficiency and total efficiency of metasurface antenna A-1 and antenna array A-8.

either simulated or measured results are in good agreement with that of the single antenna A-1. We also compare the peak gain of metasurface antenna A-1 and metasurface antenna array A-8 by simulation. Compared to the antenna A-1, the gain of antenna array A-8 has been apparently enhanced, as shown in Fig.11(a). It can be seen that the average gain of antenna array A-8 is 25.2 dB, which is larger than that of single antenna A-1 with 9.2 dB. At $f = 12.5$GHz, the realized gain reaches its maximum with 27.5 dB. The total efficiency of antenna array A-8 exceeds 80% almost in the whole working frequency range, as shown in Fig.11(b). Furthermore, the radiation efficiency of antennas array is nearly the same as the antenna A-1. Therefore, the antenna array A-8 also has a high efficiency property.

V. CONCLUSION

We propose and demonstrate a method of achieving wide-angle frequency scanning metasurface antenna and antenna array fed by spoof plasmonic waveguide. With the modulation of constant phase gradient supplied by TPGM, SSPP on the CMS can be decoupled and directionally radiated out. The wideband and wide-angle frequency scanning metasurface antenna can be achieved by independently designing of the spoof plasmonic waveguide and wideband TPGM. Both the simulated and measured results verify the working principle. The proposed metasurface antenna works in a wideband from 6.8 to 14 GHz, and the beam can scan not only in the forward directions but also in the backward directions, in which the scan angle reaches 55°. The total efficiency of the designed antenna can exceed 80% and the highest total efficiency of antenna can achieve 92%. Furthermore, such proposed antenna can be used to design antenna array with a simple feed network. An antenna array composed of eight single antennas is demonstrated by both simulation and experiment. Both the simulated and measured results show that the average gain of antenna array is obviously enhanced, and other properties of the antenna array are nearly the same with the single antenna. Since the frequency scanning metasurface antenna is based on phase gradient modulation on SSPP, our method can be effective for designing conformal antennas without open stop-band phenomena.

REFERENCES

[1] H. Raether, *Surface Plasmons on Smooth and Rough Surfaces and on Gratings*. Berlin, Germany: Springer, 1988.
[2] A. L. Stepanov, J. R. Krenn, H. Ditlbacher, A. Hohenau, A. Drezet, B. Steinberger, A. Leitner, and F. R. Aussenegg, "Quantitative analysis of surface plasmon interaction with silver nanoparticles," *Opt. Lett.*, vol. 30, no. 12, pp. 1524–1526, Jun. 2005.
[3] W. L. Barnes, A. Dereux, and T. W. Ebbesen, "Surface plasmon subwavelength optics," *Nature*, vol. 424, no. 6950, pp. 824–830, Aug. 2003.
[4] S. Zhang, K. Bao, N. J. Halas, H. Xu, and P. Nordlander, "Substrate-induced fano resonances of a plasmonic nanocube: A route to increased-sensitivity localized surface plasmon resonance sensors revealed," *Nano Lett.*, vol. 11, no. 4, pp. 1657–1663, Apr. 2011.
[5] D. K. Gramotnev and S. I. Bozhevolnyi, "Plasmonics beyond the diffraction limit," *Nature Photon.*, vol. 4, no. 2, pp. 83–91, Feb. 2010.
[6] J. B. Pendry, "Mimicking surface plasmons with structured surfaces," *Science*, vol. 305, no. 5685, pp. 847–848, Aug. 2004.
[7] Y. Han, Y. Li, H. Ma, J. Wang, D. Feng, S. Qu, and J. Zhang, "Multibeam antennas based on spoof surface plasmon polaritons mode coupling," *IEEE Trans. Antennas Propag.*, vol. 65, no. 3, pp. 1187–1192, Mar. 2017.
[8] Y. Li, J. Zhang, S. Qu, J. Wang, M. Feng, J. Wang, and Z. Xu, "K-dispersion engineering of spoof surface plasmon polaritons for beam steering," *Opt. Express*, vol. 24, no. 2, pp. 842–852, 2016.
[9] Y. Pang, J. Wang, H. Ma, M. Feng, S. Xia, Z. Xu, and S. Qu, "Extraordinary transmission of electromagnetic waves through sub-wavelength slot arrays mediated by spoof surface plasmon polaritons," *Appl. Phys. Lett.*, vol. 108, pp. 194101-1–194101-5, Apr. 2016.
[10] H. F. Ma, X. Shen, Q. Cheng, W. X. Jiang, and T. J. Cui, "Broadband and high-efficiency conversion from guided waves to spoof surface plasmon polaritons," *Laser Photon. Rev.*, vol. 8, no. 1, pp. 146–151, Jan. 2014.
[11] J. Y. Yin, J. Ren, Q. Zhang, H. C. Zhang, Y. Q. Liu, Y. B. Li, X. Wan, and T. J. Cui, "Frequency-controlled broad-angle beam scanning of patch array fed by spoof surface plasmon polaritons," *IEEE Trans. Antennas Propag.*, vol. 64, no. 12, pp. 5181–5189, Dec. 2016.
[12] J. Wang, S. Qu, H. Ma, Z. Xu, A. Zhang, H. Zhou, H. Chen, and Y. Li, "High-efficiency spoof plasmon polariton coupler mediated by gradient metasurfaces," *Appl. Phys. Lett.*, vol. 101, pp. 201104-1–201104-4, Oct. 2012.

[13] Y. Li, J. Zhang, S. Qu, J. Wang, H. Chen, Z. Xu, and A. Zhang, "Wideband radar cross section reduction using two-dimensional phase gradient metasurfaces," *Appl. Phys. Lett.*, vol. 104, pp. 221110-1–221110-7, May 2014.
[14] W. Sun, Q. He, S. Sun, and L. Zhou, "High-efficiency surface plasmon meta-couplers: Concept and microwave-regime realizations," *Light, Sci. Appl.*, vol. 5, no. 1, Jan. 2016, Art. no. e16003.
[15] H. Chen, H. Ma, J. Wang, Y. Li, M. Feng, Y. Pang, M. Yan, and S. Qu, "Broadband spoof surface plasmon polariton couplers based on transmissive phase gradient metasurface," *J. Phys. D, App. Phys.*, vol. 50, no. 37, pp. 375104-1–375104-7, 2017.
[16] L. Liu, M. Chen, J. Cai, X. Yin, and L. Zhu, "Single-beam leaky-wave antenna with lateral continuous scanning functionality based on spoof surface plasmon transmission line," *IEEE Access*, vol. 7, pp. 25225–25231, 2019.
[17] G. S. Kong, H. F. Ma, B. G. Cai, and T. J. Cui, "Continuous leaky-wave scanning using periodically modulated spoof plasmonic waveguide," *Sci. Rep.*, vol. 6, no. 1, Sep. 2016, Art. no. 29600.
[18] Y. Han, J. Wang, Y. Li, S. Gong, J. Zhang, and S. Qu, "A frequency-scanning antenna based on hybridization of the quasi-TEM mode and spoof surface plasmon polaritons mode," *J. Phys. D, Appl. Phys.*, vol. 52, no. 38, Sep. 2019, Art. no. 38LT01.
[19] D. Wei, J. Li, J. Yang, Y. Qi, and G. Yang, "Wide-scanning-angle leaky-wave array antenna based on microstrip SSPPs-TL," *IEEE Antennas Wireless Propag. Lett.*, vol. 17, no. 8, pp. 1566–1570, Aug. 2018.
[20] S.-D. Xu, D.-F. Guan, Q. Zhang, P. You, S. Ge, X.-X. Hou, Z.-B. Yang, and S.-W. Yong, "A wide-angle narrowband leaky-wave antenna based on substrate integrated waveguide-spoof surface plasmon polariton structure," *IEEE Antennas Wireless Propag. Lett.*, vol. 18, no. 7, pp. 1386–1389, Jul. 2019.
[21] Y. Zhang, H. Wang, and D. Liao, "A unidirectional beam-scanning antenna excited by corrugated metal-insulator-metal ground supported spoof surface plasmon polaritons," *IEEE Access*, vol. 7, pp. 36481–36488, 2019.
[22] N. Yu, P. Genevet, M. A. Kats, F. Aieta, J.-P. Tetienne, F. Capasso, and Z. Gaburro, "Light propagation with phase discontinuities: Generalized laws of reflection and refraction," *Science*, vol. 334, no. 6054, pp. 333–337, Oct. 2011.
[23] H. Wang, Y. Li, H. Chen, Y. Han, S. Sui, Y. Fan, Z. Yang, J. Wang, J. Zhang, S. Qu, and Q. Cheng, "Multi-beam metasurface antenna by combining phase gradients and coding sequences," *IEEE Access*, vol. 7, pp. 62087–62094, 2019.
[24] H. Wang, Y. Li, Y. Han, S. Sui, J. Wang, and S. Qu, "A circular-polarized metasurface planar reflector antenna based on pancharatnam-berry phase," *Appl. Phys. A, Solids Surf.*, vol. 125, no. 4, Apr. 2019, Art. no. 274.
[25] J. J. Xu, H. C. Zhang, Q. Zhang, and T. J. Cui, "Efficient conversion of surface-plasmon-like modes to spatial radiated modes," *Appl. Phys. Lett.*, vol. 106, no. 2, Jan. 2015, Art. no. 021102.
[26] J. J. Xu, J. Y. Yin, H. C. Zhang, and T. J. Cui, "Compact feeding network for array radiations of spoof surface plasmon polaritons," *Sci. Rep.*, vol. 6, no. 1, Sep. 2016, Art. no. 22692.
[27] Y. Fan, J. Wang, H. Ma, J. Zhang, D. Feng, M. Feng, and S. Qu, "In-plane feed antennas based on phase gradient metasurface," *IEEE Trans. Antennas Propag.*, vol. 64, no. 9, pp. 3760–3765, Sep. 2016.
[28] Y. Fan, J. Wang, Y. Li, J. Zhang, S. Qu, Y. Han, and H. Chen, "Frequency scanning radiation by decoupling spoof surface plasmon polaritons via phase gradient metasurface," *IEEE Trans. Antennas Propag.*, vol. 66, no. 1, pp. 203–208, Jan. 2018.
[29] H. Chen, H. Ma, Y. Li, J. Wang, Y. Han, M. Yan, and S. Qu, "Wideband frequency scanning spoof surface plasmon polariton planar antenna based on transmissive phase gradient metasurface," *IEEE Antennas Wireless Propag. Lett.*, vol. 17, no. 3, pp. 463–467, Mar. 2018.
[30] H. Chen, H. Ma, J. Wang, S. Qu, Y. Pang, M. Yan, and Y. Li, "Ultra-wideband transparent 90° polarization conversion metasurfaces," *Appl. Phys. A, Solids Surf.*, vol. 122, no. 4, p. 463, Apr. 2016.

HONGYA CHEN received the B.S. degree in physics from National Defense Science and Technology University, Changsha, China, in 2006, and the M.S. degree in optics engineering and the Ph.D. degree in physical electronics from Air Force Engineering University, Xi'an, China, in 2009 and 2017, respectively. Since 2007, she has been with Air Force Engineering University, where she is currently a Lecturer of physic electronics. Her current research interests include polarized metasurface, spoof surface plasmon polaritons, and design of metamaterials.

YAJUAN HAN received the B.S. degree in electrical engineering and automation from the Hefei University of Technology, Hefei, Anhui, China, in 2012, and the M.S. degree in electronic science and technology from Air Force Engineering University, Xi'an, China, in 2017. She is currently pursuing the Ph.D. degree in physical electronics with Xidian University. Her research interests include metasurface, spoof surface plasmon polaritons, and antenna design.

HUA MA received the B.S. degree in physics from the National University of Defense Technology, Changsha, China, in 1997, the M.S. degree in optics engineering from Xi'an Electronic and Technology University, Xi'an, China, in 2006, and the Ph.D. degree in physical electronics from Air Force Engineering University, Xi'an, in 2009. Since 1997, he has been with Air Force Engineering University, where he is currently a Professor of physical electronics. His current research interests include methods of collimating laserdiode beams, characteristics of photonic crystals, and design of metamaterials.

JIAFU WANG (Member, IEEE) received the B.S. degree in radar engineering, the M.S. degree in optics engineering, and the Ph.D. degree in physical electronics from Air Force Engineering University, in 2004, 2007, and 2010, respectively. Since 2007, he has been engaged in the research of electromagnetic metamaterials. His current research interests include metamaterials, metasurfaces, spoof surface plasmon polaritons, electromagnetic windows, antenna design, and other metamaterial-inspired microwave devices.

MINGBAO YAN received the B.S. and M.S. degrees in physics from Qufu Normal University, Qufu, China, in 2005 and 2008, respectively, and the Ph.D. degree in physical electronics from Air Force Engineering University, Xi'an, Shaanxi, China, in 2016. Since 2008, he has been with Air Force Engineering University, where he is currently an Associate Professor of physical electronics. His current research interests include frequency selective surface, design of stealth radome, and meta-materials.